MOLDOVA STATE UNIVERSITY

DOCTORAL SCHOOL OF NATURAL SCIENCES

Manuscript

C.Z.U.: 537.311.322:539.26:535.84:535.37:621.383.51(043.2)

BATÎR VALENTIN

TRANSPORT, VIBRATIONAL AND OPTICAL PROPERTIES OF $Cu_2(Zn,Cd)(Sn,Ge)S_4$ SOLID SOLUTIONS

134.01 – Physics and technology of materials

Summary of the doctoral thesis in physical sciences

Chisinău 2026

The PhD thesis was elaborated in the Laboratory of Materials for Photovoltaics and Photonics, Institute of Applied Physics of Moldova State University. The doctoral studies were carried out at the Doctoral School of Natural Sciences at Moldova State University.

Scientific supervisor-

ARUȘANOV Ernest	Academician, PhD Habilitate in physico-mathematical sciences, full professor, Institute of Applied Physics (IAP), Moldova State University (MSU)

Doctoral Commission:

ȚURCAN Vladimir	Corresponding member of the ASM, PhD Habilitate in physico-mathematical sciences, associate professor researcher, IAP, MSU - **president of the Doctoral Commission**
ARUȘANOV Ernest	Academician, PhD Habilitate in physico-mathematical sciences, full professor, IAP, MSU - **scientific supervisor**
CULIUC Leonid	Academician, PhD Habilitate in physico-mathematical sciences, full professor, IAP, MSU - **official reviewer**
URSACHI Veaceslav	Academician, PhD Habilitate in physico-mathematical sciences, corresponding member of the ASM, associate professor researcher, Academy of Sciences of Moldova - **official reviewer**
POSTOLACHI Valentina	PhD in physico-mathematical sciences, associate professor, "Ion CREANGĂ" State Pedagogical University of Chisinau - **official reviewer**

The dissertation defense will take place on 23.09.2026, at 14^{00} within the meeting of the Doctoral Commission of the Doctoral School of Natural Sciences, Moldova State University.

Location – Moldova State University, M. Kogălniceanu St. 65 A, Block 3, room 231, MD-2009, Chisinău, Moldova.

The doctoral thesis and its summary may be consulted at the National Library of the Republic of Moldova, the Central Library of Moldova State University (MD 2009, Chisinău, Alexei Mateevici St. 60), and on the ANACEC website (http://www.anacec.md).

The summary was sent out on "____"_____ 2026

President of the Doctoral Commission
corresponding member of the ASM, PhD Habilitate in physico-mathematical sciences, associate professor researcher _____ **ȚURCAN Vladimir**

Scientific Supervisor
PhD Habilitate in physico-mathematical sciences, full professor _____ **ARUȘANOV Ernest**

Author: _____ **BATÎR Valentin**

Contents

Conceptual foundations of the research

Relevance and importance of the topic

In the context of rising global energy consumption and limited fossil resources, the development of alternative energy sources is becoming a major priority. Solar energy is one of the most promising solutions, yet the efficiency and cost of photovoltaic devices depend directly on the properties of the semiconductor materials used.

Silicon-based photovoltaic technology currently dominates the market, but it has limitations related to the indirect band gap of the silicon and the difficulty of integrating it into flexible applications. For this reason, special interest is given to thin-film solar cell materials with a direct band gap and a high absorption coefficient. These include the compounds $Cu(In,Ga)Se_2$, $CuInSe_2$ and CdTe, although their use is limited by the high cost and toxicity of their constituent elements. These difficulties justify research into alternative materials based on more abundant and less toxic elements.

In this context, the quaternary compounds $Cu_2B^{II}C^{IV}X_4$, in particular Cu_2ZnSnS_4, Cu_2CdSnS_4 and their derivatives, are of considerable scientific and applied interest. The compound Cu_2ZnSnS_4 stands out for its use of relatively abundant elements, a band-gap width close to the optimum range for photovoltaic conversion, and a high absorption coefficient ($\sim 10^4$ cm^{-1}). Nevertheless, the performance of kesterite-based devices is limited by the formation of secondary phases, structural disorder, and the Cu_{Zn} and Zn_{Cu} antisite defects, which act as recombination centers and reduce conversion efficiency.

To overcome these limitations, cationic substitution strategies have been proposed. Partial or total substitution of zinc with cadmium allows the structural and electronic properties to be tuned, influencing the stability of the main phase and the defect concentration. Substitution of tin with germanium contributes to improved structural quality and optimized optical properties. Consequently, the systematic study of the $Cu_2(Zn,Cd)(Sn,Ge)S_4$ solid solutions is important both from a fundamental and from an applied standpoint.

Aim and objectives of the thesis

The main aim consists in studying the transport, vibrational and optical properties of the $Cu_2(Zn,Cd)(Sn,Ge)S_4$ compounds and establishing the correlation between the physico-chemical parameters and the chemical composition of the samples. The research covers both crystalline samples

and thin films, seeking to complement the existing literature and to highlight the potential of these compounds for photovoltaic and optoelectronic applications.

The objectives address three main directions. The first objective consists in determining the predominant electrical transport mechanisms in the $Cu_2(Zn,Cd)SnS_4$ solid solutions at different temperatures, important for understanding conduction in materials with localized states and hopping-type mechanisms. The second objective consists in measuring and analyzing the Raman spectra of the $Cu_2(Zn,Cd)SnS_4$ and $Cu_2(Zn,Cd)GeS_4$ compounds, in order to study their vibrational properties, identify secondary phases and assess structural quality. The third objective aims to establish the optical parameters and transitions in Cu_2ZnSnS_4 and Cu_2CdSnS_4 based on reflectance, transmittance and photoluminescence spectra, including at low temperatures.

Scientific novelty of the results

A first original element is the investigation of the transport properties of the $Cu_2(Zn,Cd)SnS_4$ solid solutions across the entire compositional range $0 \leq x \leq 1$, allowing the continuous evolution of the transport parameters to be tracked as the Cd/(Zn+Cd) ratio changes. By applying the NNH and Mott VRH models, the work contributes to clarifying the role of localized states in the electrical transport of these materials.

A second novel element consists in the use of Raman modes for composition evaluation and the proposal of a linear model for its fast estimation – an important contribution to the non-destructive characterization of kesterite materials, particularly useful for thin films.

Another original result is the identification and analysis of type-A and type-B excitons in the Cu_2CdSnS_4 compound, based on photoluminescence and reflectance spectra at low temperatures, contributing to the understanding of the band structure of Cd-containing quaternary compounds.

Applied value of the work

The theoretical significance lies in extending the knowledge of the fundamental properties of kesterite- and stannite-type compounds, while the applied value consists in the possibility of using the results to optimize the composition of the absorber layers in photovoltaic devices. By determining the transport parameters, analyzing the vibrational modes, and highlighting the optical transitions, the thesis provides important benchmarks for the design of materials with controlled properties, with potential use in thin-film solar cells and modern optoelectronic applications.

Content of the thesis

The doctoral thesis is structured into four main chapters, preceded by an introduction and followed by general conclusions and a bibliography. The content of the thesis logically follows the overall research objective, namely establishing the correlation between the chemical composition of the $Cu_2(Zn,Cd)(Sn,Ge)S_4$ compounds and their transport, vibrational and optical properties. The work contains substantial experimental and illustrative material, including 50 figures, 18 tables and 44 formulas, allowing a systematic presentation of the obtained results and their interpretation in relation to the theoretical models used in semiconductor physics and materials science.

In the ***Introduction***, the relevance and importance of the $Cu_2(Zn,Cd)(Sn,Ge)S_4$ quaternary compounds as semiconductor materials for applications in renewable energy and optoelectronics is argued. The aim and objectives of the work are formulated, targeting the investigation of the transport, vibrational and optical properties of the compounds under study, together with a brief description of the samples used in the measurements.

In the ***first chapter*** of the thesis, the main physico-chemical properties of the $Cu_2(Zn,Cd)(Sn,Ge)S_4$ quaternary compounds are analyzed, and the results obtained worldwide with a view to their application in photovoltaic and photoelectrochemical devices are presented.

The applications of the CZTSSe quaternary compounds as absorber layers in photovoltaic cells are described, for which a record efficiency of 14.9% [1] has been achieved, as well as in photoelectrochemical devices for hydrogen production. The strategic advantage of these materials compared to indium- or gallium-based compounds is highlighted, owing to the abundance and low cost of their constituent elements, along with the prospects for improving efficiency relative to the theoretical Shockley-Queisser limit.

A description of the kesterite and stannite structural types is presented, differentiated by the arrangement of the cationic planes, and the higher energetic stability of the kesterite-type structure is indicated. Special attention was given to intrinsic structural defects – copper vacancies (V_{Cu}) and the Cu_{Zn}/Zn_{Cu} antisite defects – whose formation is favored by Cu-deficient and Zn-rich conditions, correlated with photovoltaic efficiencies greater than 8%.

The transport properties of the quaternary compounds are presented, characterized by an activation-type behavior determined by the presence of different electrical conduction mechanisms, activated depending on the temperature of the investigated sample. Thus, the variable-range hopping

conduction mechanisms of the Mott and Shklovskii-Efros type are described, together with the acceptor-band model used to interpret the Anderson metal-insulator transition.

The vibrational properties were investigated by means of Raman spectroscopy, a method that allows the identification of the crystal structure, estimation of the chemical composition, and detection of secondary phases. This chapter presents the positions of the main Raman modes characteristic of compounds with kesterite, stannite and wurtzstannite structures, as well as the uni-modal, bi-modal and tri-modal behavior of the peaks in the solid solutions.

The optical properties and excitons were analyzed using the absorption, transmittance and photoluminescence spectra of the $Cu_2Zn_{1-x}Cd_xSnS_4$ solid solutions reported in the specialized literature. Thus, the quasi-linear dependence of the band gap on composition was presented, ranging between 1.35 eV (CZTS) and 1.14 eV (CCTS). Wannier-Mott-type excitons were described, with discrete energy levels located within the band gap of the material, whose small binding energy and large excitonic radius justify treating the semiconductor crystal as a continuous medium.

The second chapter is devoted to the study of the transport properties of the $Cu_2Zn_{1-x}Cd_xSnS_4$ quaternary compounds and presents the experimental analysis of the conduction mechanisms in samples of these compounds. Crystalline samples were obtained by the chemical vapor transport method, and the chemical composition was determined by X-ray fluorescence spectroscopy. The composition data are presented in Table 1, which includes the atomic concentrations of the Cu, Zn, Cd, Sn and S elements, as well as the relevant cationic ratios.

Table 1. Chemical composition of the CZCTS samples measured by the XRF method.

Sample	Cu (at. %)	Zn (at. %)	Cd (at. %)	Sn (at. %)	S (at. %)	Cd/ (Zn+Cd)	Cu/ (Zn+Cd+Sn)	(Zn+Cd) /Sn
S1	18.4±0.07	8.6±0.05	0.0±0.01	9.1±0.1	63.9±0.1	0.00	1.04	0.95
S2	18.4±0.09	7.2±0.06	1.7±0.1	9.4±0.1	63±1	0.19	1.00	0.94
S3	18.3±0.09	6.2±0.05	2.9±0.06	9.0±0.1	64±1	0.32	1.01	1.01
S4	22.4±0.2	8.6±0.1	5.3±0.1	15.8±0.3	48±1	0.38	0.75	0.88
S5	17.5±0.08	5.1±0.05	3.7±0.06	8.5±0.1	65±1	0.42	1.00	1.04
S6	19.9±0.1	2.8±0.09	6.2±0.07	10.7±0.2	60 ±2	0.69	1.01	0.84
S7	17.9±0.2	1.9±0.08	6.9±0.2	9.8±0.3	64±2	0.78	0.96	0.91
S8	19.1±0.1	0.0±0.03	11.0±0.1	12.0±0.2	57.6±0.9	1.00	0.83	0.92

From Table 1 it can be observed that samples S1, S3 and S6 show a Cu excess, while samples S4, S7 and S8 show a Cu deficit. A content close to the stoichiometric value, Cu (Cu/(Zn+Cd+Sn) ≈ 1), was observed only for samples S2 and S5. Likewise, samples S3 and S5 showed an excess of the Zn+Cd sum, while the other samples showed a deficit of these cations. In addition, deviations between

the nominal composition and the Cd/(Zn+Cd) ratio were identified for samples S2-S5, the other samples showing good agreement between these values.

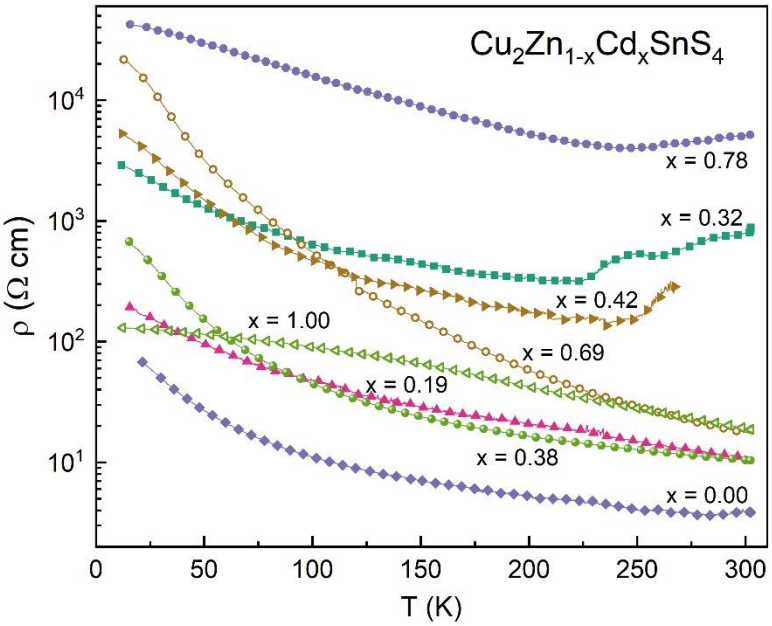

Fig. 1. Temperature dependence of resistivity in the CZCTS solid solutions.

The temperature dependences of resistivity of the $Cu_2(Zn,Cd)SnS_4$ solid solutions are shown in Fig. 1. As can be observed from this figure, all curves display an activation-type behavior in the investigated samples. Likewise, the different behavior of the *ρ(T)* curves with decreasing temperature is most likely determined by the varying proximity to the metal-insulator transition (MIT), which has been frequently observed in kesterites [2–4].

In general, the temperature dependence of resistivity for weakly doped crystalline semiconductors can be described by the following expression [5],

$$\rho(T) = A_p T^m \exp\left[\left(\frac{T_{0p}}{T}\right)^{1/p}\right] \quad (1)$$

which suggests different hopping conduction regimes. Here, A_p is a numerical constant, $p = 1$ corresponds to nearest-neighbor hopping conduction (NNH), $p = 4$ describes the Mott-type variable-range hopping conduction regime (VRH), T_{0p} represents the characteristic Mott temperature, and $m = 1/p$.

In the case of the NNH mechanism, the analysis was carried out by plotting the experimental data in the coordinates $\ln(\rho/T) = f(T^{-1})$. This assumes the use of relation (1) for the case $p = 1$, corresponding to nearest-neighbor hopping conduction. After the approximation of *ρ(T)* curves (Fig.

2), the data for ΔT_n and E_n were obtained (Table 2). These values are in good agreement with the values reported in Ref. [6] for the CZCTS solid solutions, over a smaller range of the variable *x*.

However, the best approximation of the $\rho(T)$ curves was obtained for the case $p = 4$, corresponding to the Mott-type variable-range hopping conduction (Fig. 3). In this case, the linear regions were identified in the thermal range ~56-142 K, which is consistent with the ranges reported for the same family of compounds in the literature [2, 7, 8].

The parameters determined from the analysis of the NNH and Mott-VRH models are presented in Table 2, which includes the thermal ranges ΔT_n and ΔT_M, specific to each conduction mechanism, the activation energy E_n, the characteristic temperature T_{04}, the acceptor-band half-width W, the relative acceptor concentration N/N_c, and the acceptor localization radius far from the metal-insulator transition a/a_0.

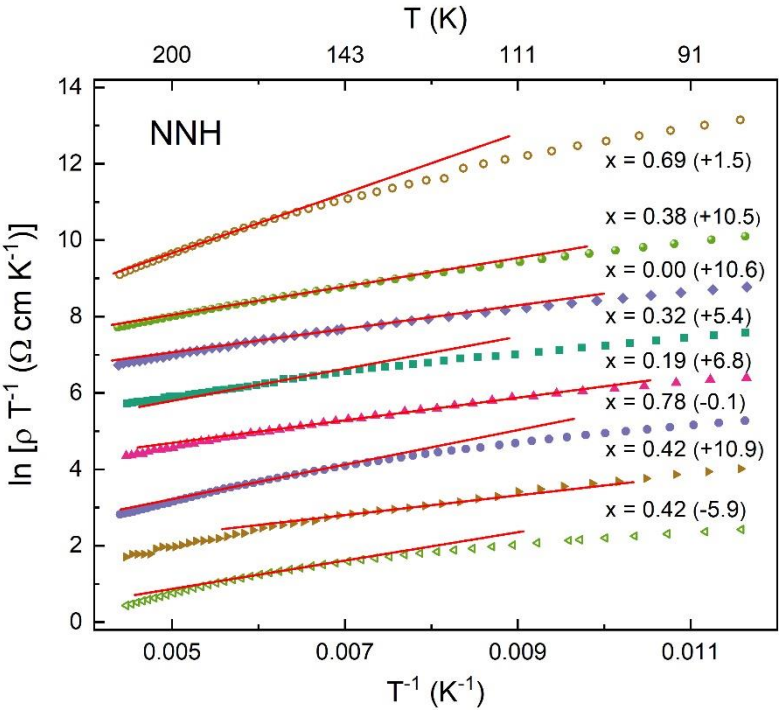

Fig. 2. Temperature dependences of resistivity in the CZCTS compounds, plotted in the form ln(ρ/T) = f(T^{-1}). For clarity, the curves are shifted vertically by the values indicated in parentheses. The linear regions are indicated with straight lines.

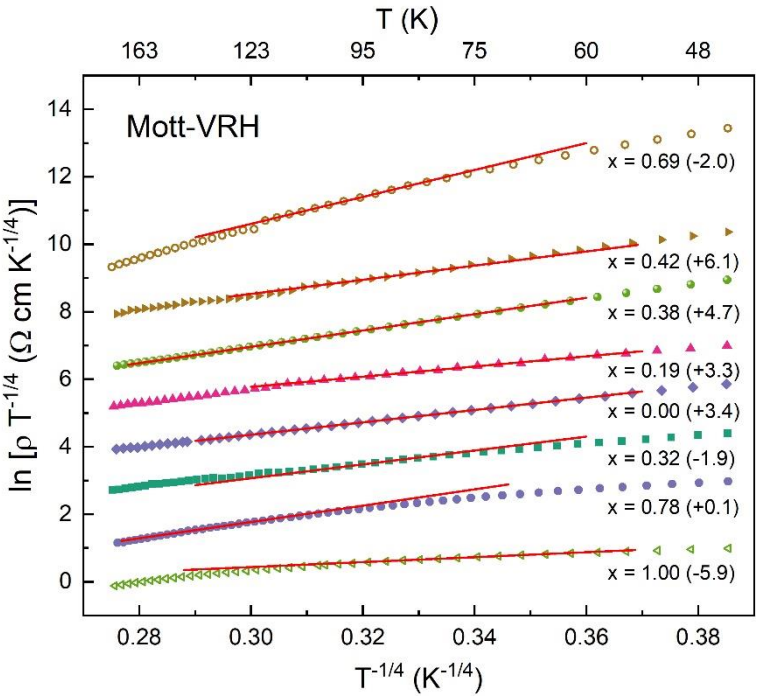

Fig. 3. Temperature dependences of resistivity in the CZCTS compounds, plotted in the form $\ln(\rho/T^{1/4}) = f(T^{-1/4})$. For clarity, the curves are shifted vertically by the values indicated in parentheses. The linear regions are indicated with straight lines.

Table 2. Width of the thermal range (ΔT_n) and activation energy (E_n) specific to the NNH mechanism. Width of the thermal range (ΔT_M) and characteristic Mott VRH temperature (T_{04}) specific to the Mott VRH mechanism; acceptor-band half-width (W), relative acceptor concentration (N/N_c), and acceptor localization radius far from the metal-insulator transition (a/a_0) calculated from the analysis of the Mott VRH transport mechanism.

Sample	ΔT_n (K)	E_n (meV)	ΔT_M (K)	$T_{04}\ 10^3$(K)	W (meV)	N/N_c	a/a_0
S1	145-165	27	72-139	112.9	32	0.59	2.5
S2	109-151	25	56-95	52.08	20	0.63	2.7
S3	158-172	36	88-100	178.8	28	0.52	2.1
S4	150-167	32	100-135	342.2	41	0.49	2.0
S5	119-148	22	77-92	193.2	27	0.51	2.0
S6	170-192	68	84-110	2533	58	0.27	1.4
S7	159-175	39	123-142	341.7	43	0.50	2.0
S8	157-163	32	75-86	2.894	9	0.80	4.9

The dependences of the parameters W and E_n on the Cd/(Zn+Cd) ratio are shown in Fig. 4, while the dependences of the parameters N/N_c and a/a_0 on the cationic ratio are shown in Fig. 5. These figures indicate a non-monotonic behavior of the mentioned parameters, suggesting that the electrical properties of the $Cu_2(Zn,Cd)SnS_4$ solid solutions are not determined solely by the Cd/(Zn+Cd) ratio, but are strongly influenced by the defect concentration and structural disorder. Sample S6, characterized by the ratio (Zn+Cd)/Sn ≈ 0.84 and by the large value of the acceptor-band half-width

$W \approx 58$ meV, is interpreted as having the highest level of structural disorder, associated with the formation of Cu_{Zn} antisite defects, which act as acceptors. Thus, for most samples the values of W and E_n are comparable, indicating that the Fermi level is positioned near the edge of the acceptor band and allowing both hopping conduction regimes to be observed.

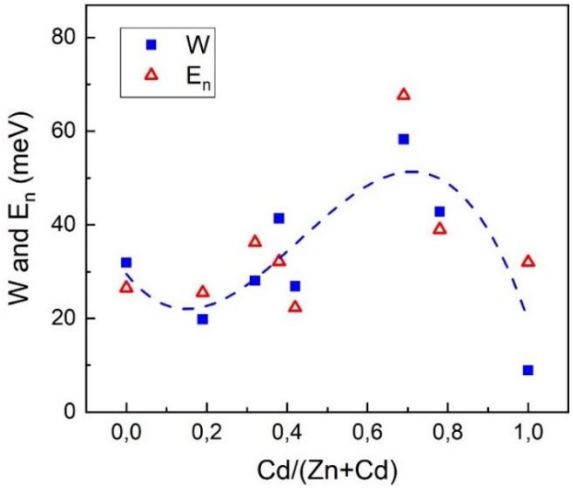

Fig. 4. Dependences of the parameters *W* and E_n on the Cd/(Zn+Cd) ratio.

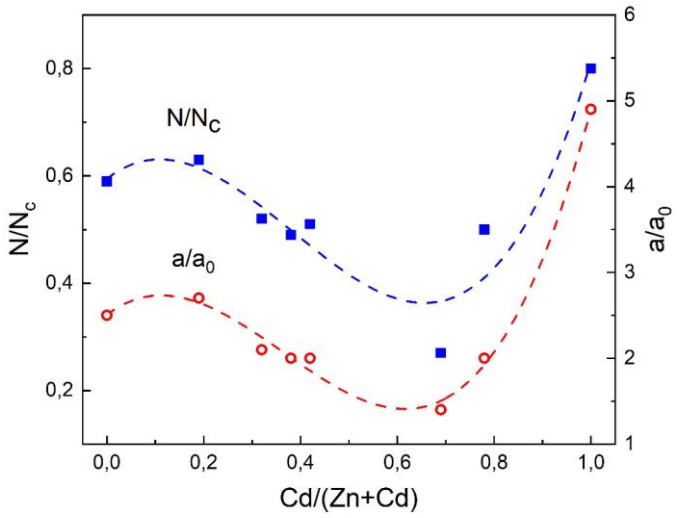

Fig. 5. Dependences of the parameters N/N_c and a/a_0 on the Cd/(Zn+Cd) ratio.

The third chapter of the doctoral thesis is devoted to the Raman characterization of the $Cu_2(Zn,Cd)SnS_4$ and $Cu_2(Zn,Cd)GeS_4$ solid solutions. The Raman spectra of the crystalline $Cu_2(Zn,Cd)SnS_4$ samples were measured at 300 K with excitation wavelengths of 532 nm and 785 nm. The chemical composition of the samples is presented in Table 3, which includes the atomic concentrations and cationic ratios. Thus, a Cu surplus (Cu/(Zn+Cd+Sn) > 1) is observed for samples Cd 0.0, Cd 0.4 and Cd 0.7, while for samples Cd 0.5, Cd 0.6 and those with a Cd/(Zn+Cd) ratio > 0.7

a Cu deficit was identified. The only samples for which the ratio Cu/(Zn+Cd+Sn) ≈ 1 are Cd 0.3 and Cd 0.5_1.

Table 3. Chemical composition of the CZCTS solid solutions.

Sample	Cu (at. %)	Zn (at. %)	Cd (at. %)	Sn (at. %)	S (at. %)	Cd/ (Zn+Cd)	Cu/ (Zn+Cd+Sn)	(Zn+Cd) /Sn
Cd 0.0	18.4±0.07	8.6±0.05	0.0±0.01	9.1±0.1	63.9±0.1	0.00	1.04	0.95
Cd 0.3	18.4±0.09	7.2±0.06	1.7±0.1	9.4±0.1	63±1	0.19	1.00	0.94
Cd 0.4	18.3±0.09	6.2±0.05	2.9±0.06	9.0±0.1	64±1	0.32	1.01	1.01
Cd 0.5	22.4±0.2	8.6±0.1	5.3±0.1	15.8±0.3	48±1	0.38	0.75	0.88
Cd 0.5_1	17.5±0.08	5.1±0.05	3.7±0.06	8.5±0.1	65±1	0.42	1.00	1.04
Cd 0.6	18.3±0.1	4.4±0.06	4.8±0.1	10.0±0.2	63±1	0.52	0.95	0.92
Cd 0.7	19.9±0.1	2.8±0.09	6.2±0.07	10.7±0.2	60±2	0.69	1.01	0.84
Cd 0.8	18.3±0.1	2.4±0.04	7.6±0.3	10.6±0.2	61±1	0.76	0.89	0.94
Cd 0.8_1	17.9±0.2	1.9±0.08	6.9±0.2	9.8±0.3	64±2	0.78	0.96	0.91
Cd 1.0	20.3±0.1	0.0±0.04	14.6±0.2	16.3±0.2	49±1	1.00	0.66	0.90
Cd 1.0_1	19.1±0.1	0.0±0.03	11.0±0.1	12.0±0.2	57.6±0.9	1.00	0.83	0.92
Cd 1.0_2	17.2±0.07	0.0±0.02	9.1±0.08	9.6±0.1	64±0.8	1.00	0.92	0.96

The Raman spectra of the CZCTS solid solutions excited with a wavelength of 532 nm are shown in Fig. 6, and the positions of the most intense peaks are indicated in Table 4. For the CZTS compound, corresponding to the ratio Cd/(Zn+Cd) = 0.00, the Raman spectrum is characteristic of the kesterite-type structure, with the space group $I\bar{4}$. The phonon modes at the center of the Brillouin zone are described by the irreducible representation:

$$\Gamma = 3A \oplus 7B \oplus 7E, \quad (2)$$

where the modes $3A \oplus 6B \oplus 6E$ are Raman active, while the 6B $\oplus$ 6E modes are also IR active. The CZTS spectrum shows an intense peak at ~338 cm^{-1}, accompanied by prominent peaks at 287, 351 and 250 cm^{-1}. The peaks located at 287 and 338 cm^{-1} were assigned to A-symmetry modes, determined by the vibrations of the sulfur atoms in the kesterite-type structure, while the peaks at 351 and 250 cm^{-1} were associated with B and E modes.

The compound Cu_2CdSnS_4 (CCTS), corresponding to the ratio Cd/(Zn+Cd) = 1.00, crystallizes in the stannite-type structure, space group $I\bar{4}2m$ (D_{2d}^{11}). The irreducible representation of the phonon modes in the stannite-type structure is as follows:

$$\Gamma = 2A_1 \oplus A_2 \oplus 2B_1 \oplus 4B_2 \oplus 6E, \quad (3)$$

In this expression, the A_1, B_1, B_2 and E modes are Raman active, the B_2 and E modes are also IR active, while the A_2 mode is considered silent. The CCTS spectrum shows intense peaks at 332, 284, 239, 344 and 364 cm^{-1}. The peaks located at 332 and 284 cm^{-1} were assigned to the A_1 modes,

associated with anion vibrations, while the peaks positioned at 239, 344 and 364 cm^{-1} correspond to the E and B_2 modes.

For samples with intermediate composition, the Raman spectra indicate the presence of both quaternary-phase modes and secondary-phase modes. Samples with Cd/(Zn+Cd) = 0.32 and 0.38 show a peak at ~304 cm^{-1}, associated with the cubic Cu_2SnS_3 phase, while the sample with Cd/(Zn+Cd) = 0.69 shows a peak at ~314 cm^{-1}, assigned to the SnS_2 phase. These observations indicate compositional and phase inhomogeneity, determined by deviations from the optimal synthesis conditions.

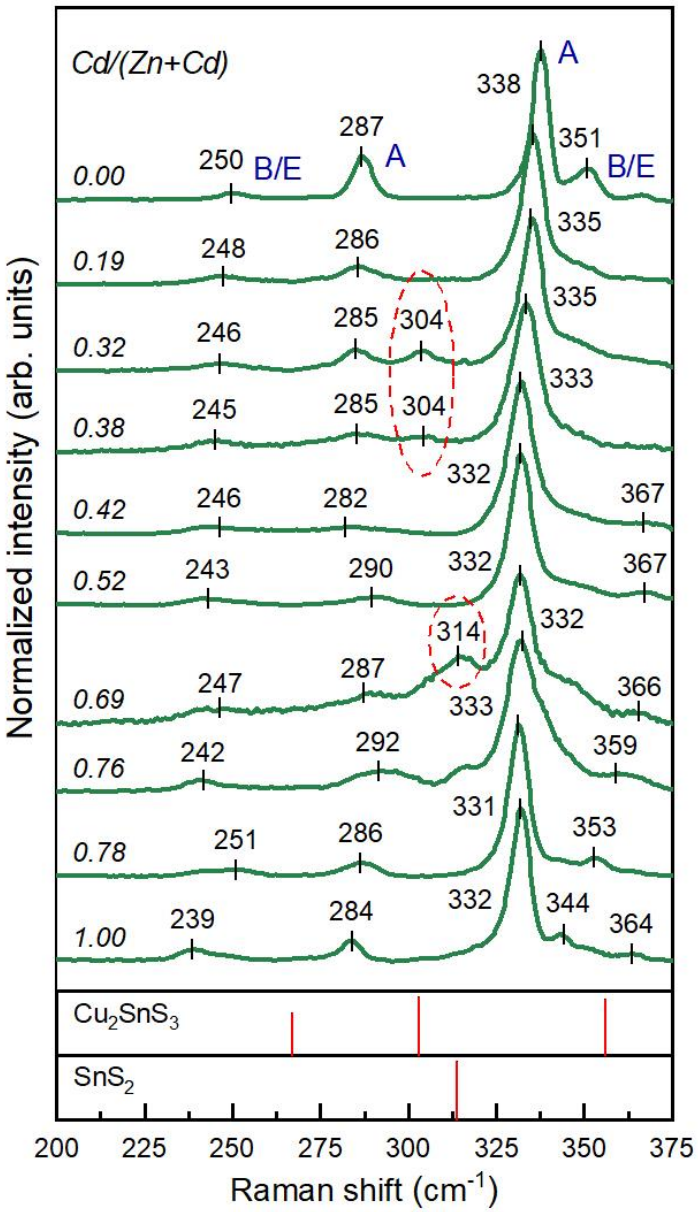

Fig. 6. Raman spectra of the CZCTS solid solutions excited with a wavelength of 532 nm (room temperature). The peaks marked with a dashed line correspond to secondary phases.

Table 4. Position of the most intense Raman peaks in the CZCTS solid solutions, excited with a wavelength of 532 nm. The main peaks are highlighted in bold.

Cd/(Zn+Cd)	Raman shift (cm^{-1})
0.00	250, 287, **338**, 351
0.19	248, 286, **335**
0.32	246, 285, **335**
0.38	245, 285, **333**
0.42	246, 282, **332**, 367
0.52	243, 290, **332**, 367
0.69	247, 287, **332**, 366
0.76	242, 292, **333**, 359
0.78	251, 286, **331**, 353
1.00	239, 284, **332**, 344, 364

A key result of the Raman analysis for the 532 nm wavelength is the shift of the main peak as the Cd/(Zn+Cd) ratio increases. As shown in Fig. 7, this dependence covers two regions. Within the first interval ($0 \leq Cd/(Zn+Cd) \leq 0.6$), the shift is described by the following expression:

$$\omega[cm^{-1}] = 338 - 11.1 \cdot \left(\frac{Cd}{Zn + Cd}\right), \quad (4)$$

Within the second interval ($0.6 \leq Cd/(Zn+Cd) \leq 1.0$), the shift of the main peak can be described using the expression:

$$\omega[cm^{-1}] = 332 + 0.335 \cdot \left(\frac{Cd}{Zn + Cd}\right), \quad (5)$$

The existence of these two regions highlights the kesterite–stannite structural transition, which occurs around the value $Cd/(Zn+Cd) \approx 0.6$ (under 532 nm excitation).

The shift of the main peak toward lower wavenumbers is determined by the mass effect and by the weaker interaction of the Cd–S bonds compared to Zn–S, as a result of the larger ionic radius of the Cd^{2+} ion compared to the Zn^{2+} ion.

The full width at half maximum (FWHM) of the main peak varies between 5.3 and 12.5 cm^{-1}, indicating a high level of crystallinity. The dependence of the FWHM on the Cd/(Zn+Cd) ratio shows a maximum at ~0.5, attributed to the structural disorder associated with the rearrangement of the cationic layers. For higher Cd concentrations, the decrease in FWHM indicates improved structural homogeneity.

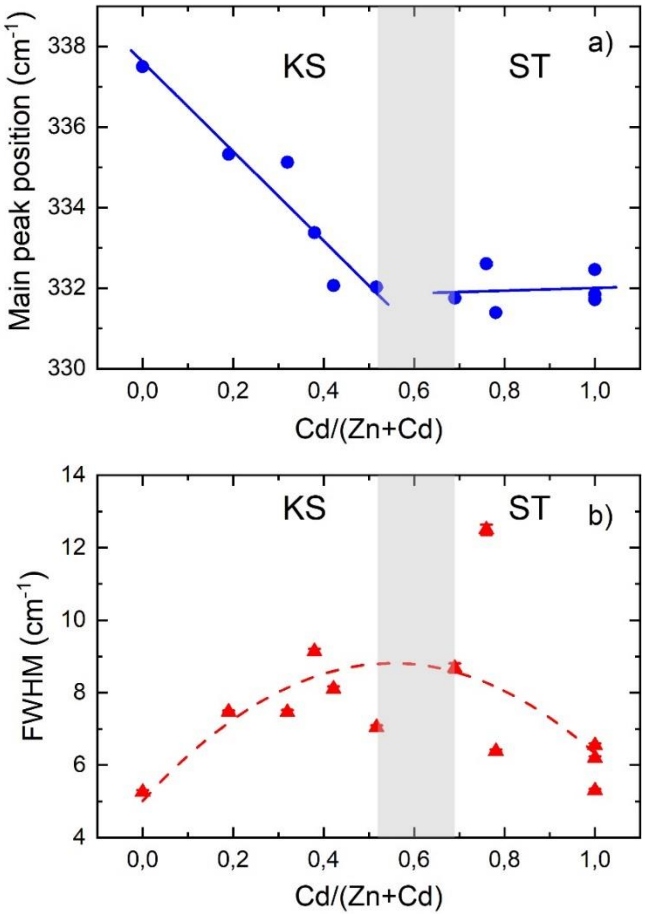

Fig. 7. a) - Raman shift and b) - full width at half maximum (FWHM) of the main peak as a function of the Cd content in the CZCTS solid solutions. The gray band indicates the kesterite–stannite transition.

The Raman spectra of the CZCTS solid solutions measured with a wavelength of 785 nm are shown in Fig. 8, and the positions of the most intense peaks are indicated in Table 5. For the 785 nm wavelength, the CZTS spectrum shows intense peaks at 285, 336, 366 and 374 cm^{-1}. The first two peaks were assigned to A-symmetry modes (kesterite-type structure), while the peaks located at 366 and 374 cm^{-1} were associated with polar E- and B-symmetry modes, enhanced by Fröhlich-type electron-phonon interaction under near-resonance excitation conditions.

For the CCTS compound excited with a wavelength of 785 nm, the spectrum shows intense peaks at 285, 313, 333 and 365 cm^{-1}. The peaks located at 285 and 333 cm^{-1} were assigned to the A_1 modes (stannite-type structure), while the peak positioned at 313 cm^{-1} was associated with the secondary SnS_2 phase. Similar peaks in the range 313–315 cm^{-1} were also identified in the samples with Cd/(Zn+Cd) = 0.69–0.78. In the samples with Cd/(Zn+Cd) = 0.32 and 0.38, the peaks detected at 316–320 cm^{-1} can be correlated with the orthorhombic secondary phase Cu_3SnS_4. The presence of

these phases confirms that the introduction of Cd can generate cationic disorder and reduce the structural stability of the quaternary phase, especially in the region of the kesterite–stannite transition.

The evolution of the main peak for the 785 nm wavelength also comprises two distinct regions (Fig. 9). The first region (Cd/(Zn+Cd) < 0.7) is characterized by a decrease in frequency with increasing Cd content, determined by the mass effect and the reduction of the Zn/Cd–S interatomic forces. The second region (Cd/(Zn+Cd) > 0.7) shows a shift toward higher wavenumbers, attributed to angular distortions of the metal-sulfur tetrahedra near the stannite region.

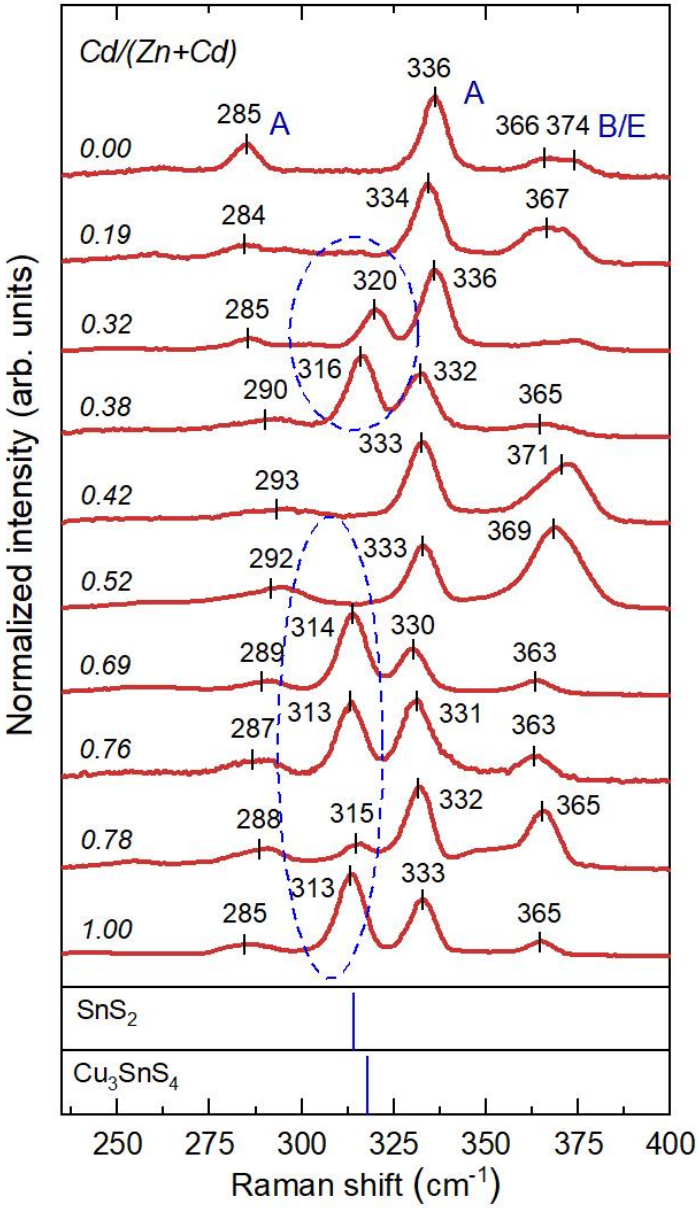

Fig. 8. Raman spectra of the CZCTS solid solutions excited with a wavelength of 785 nm (room temperature). The peaks marked with a dashed line correspond to secondary phases.

Table 5. Position of the most intense Raman peaks in the CZCTS solid solutions, obtained for a wavelength of 785 nm. The main peaks are highlighted in bold.

Cd/(Zn+Cd)	Raman shift (cm^{-1})
0.00	285, **336**, 366, 374
0.19	284, **334**, 367
0.32	285, **336**
0.38	290, **332**, 365
0.42	293, **333**, 371
0.52	292, **333**, 369
0.69	289, **330**, 363
0.76	287, **331**, 363
0.78	288, **332**, 365
1.00	285, **333**, 365

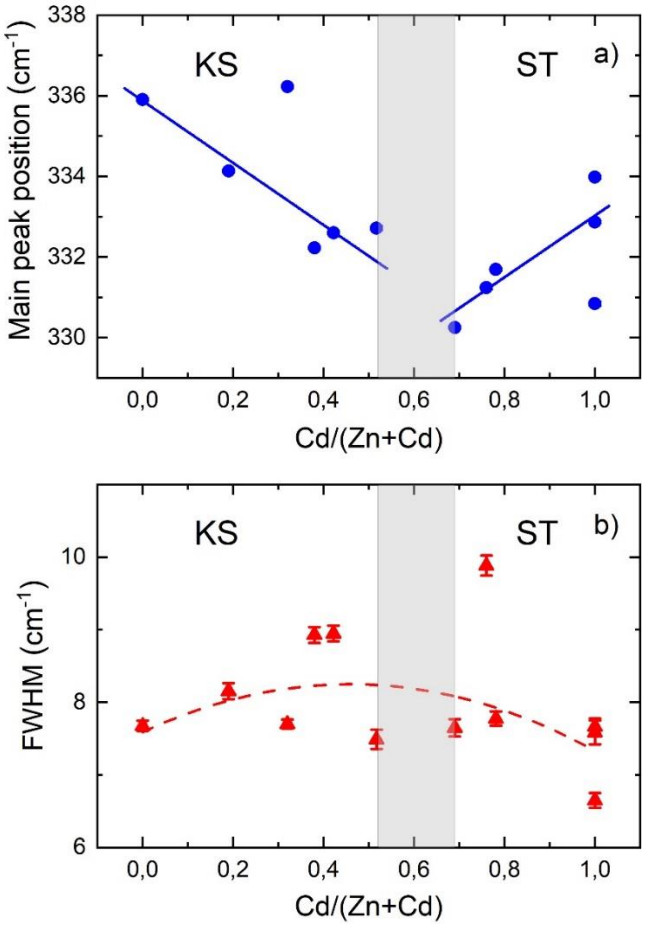

Fig. 9. a) - Raman shift and b) - full width at half maximum (FWHM) of the main peak as a function of the Cd content in the CZCTS solid solutions. The gray band indicates the kesterite–stannite transition.

The two above-mentioned regions were approximated using the expressions:

$$\omega[cm^{-1}] = 336 - 7.93 \cdot \left(\frac{Cd}{Zn + Cd}\right), \quad (6)$$

$$\omega[cm^{-1}] = 326 - 6.29 \cdot \left(\frac{Cd}{Zn + Cd}\right), \quad (7)$$

Thus, the kesterite-stannite structural transition is located at ~0.7 in the spectra obtained with the 785 nm wavelength, and at ~0.6 for the 532 nm wavelength, indicating a coexistence of the two structures in the range $0.6 \leq Cd/(Zn+Cd) \leq 0.7$.

The dependence of the FWHM parameter of the main peak in the case of the 785 nm wavelength on the Cd/(Zn+Cd) ratio is similar to the one obtained for the 532 nm wavelength, with a maximum around the value ≈ 0.5, correlated with the maximum structural disorder.

Table 6. Chemical composition of the CZCGS thin films: before (non) and after (ann) thermal annealing.

Sample	Cu (at.%)	Zn (at.%)	Cd (at.%)	Ge (at.%)	S (at.%)	Cu/ (Zn+Cd+Ge)	(Zn+Cd)/ Ge	Cd/ (Zn+Cd)
before thermal annealing								
Cd 0.00 non	21.6±0.2	14.7±0.2	0.0±0.0	13.7±0.2	50.1±0.8	0.76	1.08	0.00
Cd 0.10 non	25.3±0.2	15.7±0.1	3.2±0.6	17.7±0.2	38.1±0.6	0.69	1.07	0.17
Cd 0.25 non	26.7±0.3	13.2±0.2	3.7±0.9	16.3±0.2	40.2±0.9	0.81	1.04	0.22
Cd 0.50 non	29.8±0.2	10.7±0.1	11.2±0.7	19.6±0.2	28.7±0.5	0.72	1.12	0.51
Cd 0.75 non	29.8±0.2	5.6±0.1	18.2±0.8	18.6±0.2	27.8±0.5	0.70	1.28	0.76
Cd 0.90 non	25.8±0.2	2.0±0.08	18±1	16.4±0.2	37.5±0.6	0.71	1.23	0.90
Cd 1.00 non	26.4±0.2	0.0±0.06	21±1	16.7±0.2	36.3±0.6	0.71	1.23	1.00
after thermal annealing								
Cd 0.00 ann	21.4±0.2	14.6±0.1	0.0±0.0	13.3±0.1	50.6±0.7	0.77	1.10	0.00
Cd 0.10 ann	24.1±0.2	15.1±0.1	3.2±0.5	16.8±0.1	40.8±0.5	0.69	1.09	0.17
Cd 0.25 ann	22.7±0.2	11.4±0.1	3.4±0.6	13.8±0.1	48.8±0.6	0.79	1.07	0.23
Cd 0.50 ann	20.4±0.1	7.3±0.09	8.5±0.6	13.8±0.1	49.9±0.6	0.69	1.14	0.54
Cd 0.75 ann	20.8±0.1	3.8±0.07	13.5±0.6	12.5±0.1	49.4±0.6	0.70	1.38	0.78
Cd 0.90 ann	21.5±0.2	1.6±0.08	15±1	11.7±0.1	50.2±0.6	0.76	1.41	0.90
Cd 1.00 ann	20.9±0.1	0.0±0.04	17.2±0.7	11.7±0.1	50.2±0.7	0.72	1.47	1.00

The $Cu_2Zn_{1-x}Cd_xGeS_4$ (CZCGS) thin-film solid solutions were obtained by the spray pyrolysis method, followed by thermal annealing in a sulfur atmosphere at 525 °C for 30 minutes. The chemical composition was determined by the XRF method. Thus, all samples, both before and after thermal annealing, show a Cu deficit and a surplus of the Zn+Cd sum (Table 6). Good agreement was also observed between the nominal value of *x* and the experimental Cd/(Zn+Cd) ratio. After thermal

annealing, the sulfur concentration approached the stoichiometric value more closely, owing to sulfurization in the S_2 atmosphere.

The Raman spectra of the thermally annealed CZCGS solid solutions, measured at 300 K with a wavelength of 785 nm, are shown in Fig. 10, and the positions of the most intense peaks are collected in Table 7.

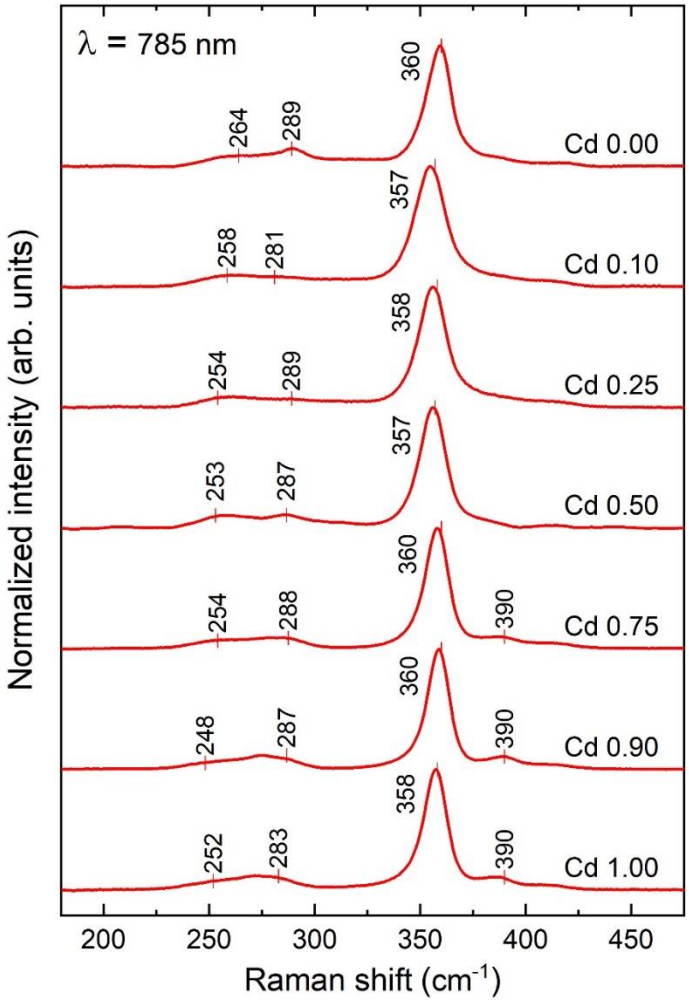

Fig. 10. Raman spectra of the CZCGS solid solutions after thermal annealing**.**

Table 7. Position of the most intense Raman peaks in the CZCGS solid solutions.

Sample	Raman shift (cm^{-1})
Cd 0.00	264, 289, **360**
Cd 0.10	258, 281, **357**
Cd 0.25	254, 289, **358**
Cd 0.50	253, 287, **357**
Cd 0.75	254, 288, **360**, 390
Cd 0.90	248, 287, **360**, 390
Cd 1.00	252, 283, **358**, 390

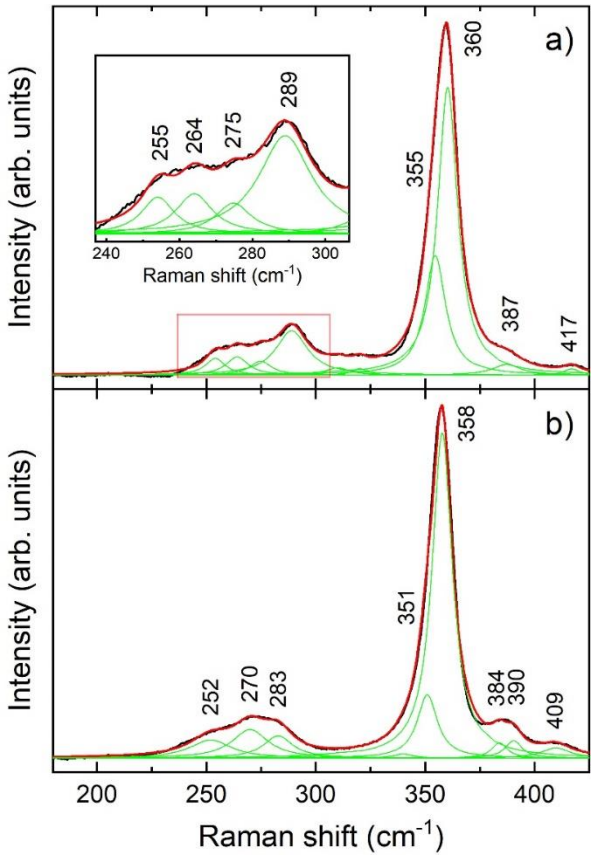

Fig. 11. Fit (red curve) of the experimental Raman spectra (black curves) using Lorentzian curves (green): a) - sample Cd 0.00 ann (CZGS) and b) - sample Cd 1.00 ann (CCGS). The inset shows the magnified peak region corresponding to the wurtzstannite-type structure in sample Cd 0.00 ann.

The compound Cu_2ZnGeS_4 (CZGS) can crystallize in either the stannite structure or the wurtzstannite-type structure, the wurtzstannite structure being more probable from an energetic standpoint [9]. Fig. 11 shows that the CZGS sample displays peaks at ~255, 264, 275 and 289 cm^{-1}, characteristic of the wurtzstannite-type structure.

For the wurtzstannite-type structure, with space group $Pmn2_1$, the irreducible representation of the phonon modes at the center of the Brillouin zone is:

$$\Gamma = 13A_1 \oplus 10A_2 \oplus 9B_1 \oplus 13B_2, \quad (8)$$

All mode types are Raman active, while the A_1, B_1 and B_2 modes are also IR active, leading to LO–TO splitting. The most intense Raman peaks for CZGS were detected at 360, 289 and 264 cm^{-1}. The peaks located at 360 and 289 cm^{-1} were assigned to the A_1 mode, associated with the vibrations of the sulfur atoms around the Ge atoms and the deformation of the Ge–S bonds.

The compound Cu_2CdGeS_4 (CCGS, sample Cd 1.00 ann) also crystallizes in the wurtzstannite-type structure, space group $Pmn2_1$ [10]. The Raman spectrum shows three prominent bands in the

region 230–370 cm^{-1}. The peaks located at 358 and 283 cm^{-1} were assigned to the A_1 mode, associated with the in-phase vibrations of the GeS_4 tetrahedra, while the peak detected at 252 cm^{-1} was associated with the A_2 mode, determined by the vibrations of the sulfur atoms.

Comparing the CZGS and CCGS spectra, the positions of the main peaks change only slightly with the variation of the Cd concentration. In contrast, the band located in the region 280–300 cm^{-1} shifts noticeably toward lower wavenumbers with increasing Cd content (Fig. 12), indicating that the vibrations of the Ge–S bonds are not directly influenced by Zn–Cd substitution, while the change in lattice parameters and the increase in interatomic distances lead to a decrease in phonon energy.

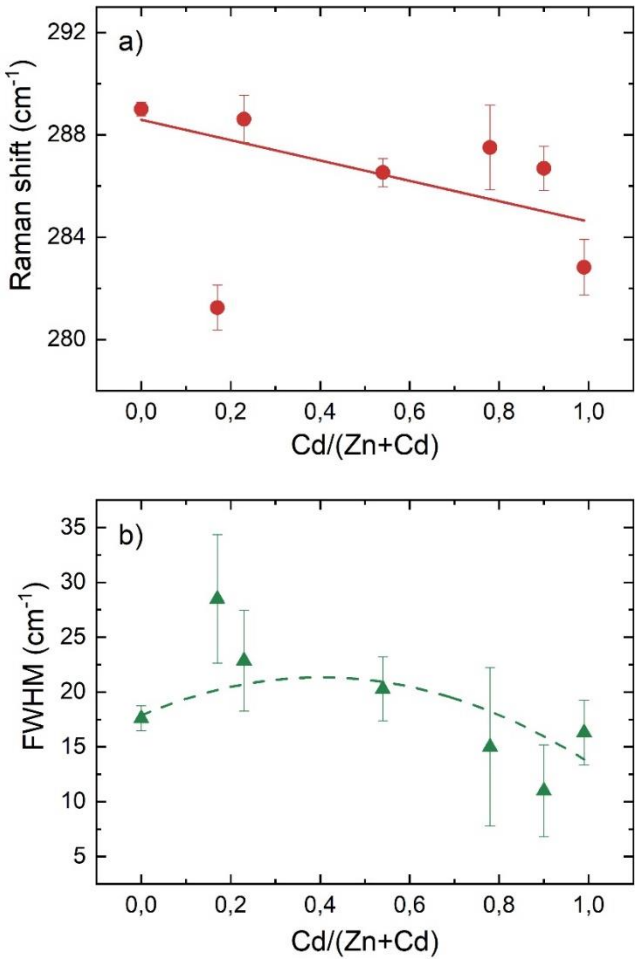

Fig. 12. a) - Raman shift and b) –width (FWHM) of the band located in the region 280–300 cm^{-1}, as a function of the Cd content in the CZCGS solid solutions.

An important application of Raman spectroscopy is the rapid estimation of the chemical composition (Fig. 12). The band in the region 280–300 cm^{-1} shows a clear dependence on the Cd/(Zn+Cd) ratio, and a linear fit yielded the relation given below.

$$\omega[cm^{-1}] = 289 - 3.97 \cdot \left(\frac{Cd}{Zn + Cd}\right), \quad (9)$$

However, the method remains approximate and may require additional calibration, since the peak position can be affected by structural defects and reduced crystallinity.

The dependence of the band width (FWHM) located in the range 280–300 cm^{-1} on the Cd/(Zn+Cd) ratio (Fig. 12) shows a maximum at ~0.3, associated with the relatively high structural disorder in samples with low Cd content. The subsequent decrease in band width indicates an improvement in crystalline quality.

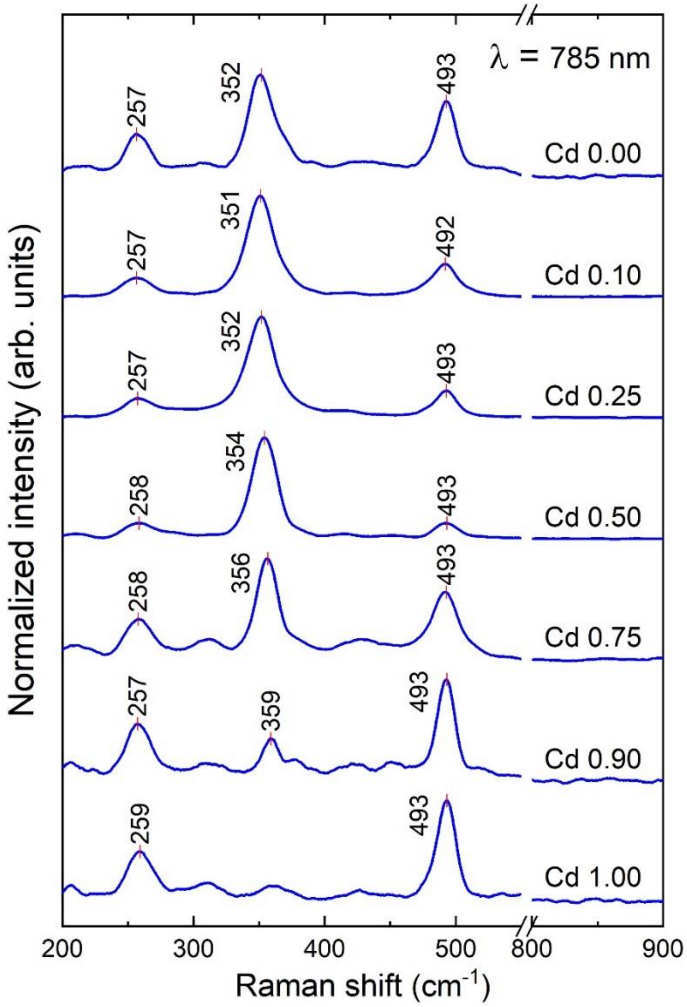

Fig. 13. Raman spectra of the CZCGS solid solutions before thermal annealing, measured at 300 K temperature.

The Raman spectra of the non-annealed samples (Fig. 13) indicate reduced structural and phase quality. The main band located in the region 351–359 cm^{-1} is shifted toward lower wavenumbers owing to the reduced crystallinity. In addition, two intense bands were observed at ~258 and 493 cm^{-1}, which do not correspond to the quaternary phase or to known secondary phases. Their disappearance after thermal annealing confirms the dissolution of the intermediate compounds formed during spraying (thiourea or CuCl) and the formation of the main quaternary phase.

The different behavior of the non-annealed samples as a function of Cd content suggests distinct mechanisms of quaternary-phase formation: for low Cd content, the quaternary phase partially forms during spraying, with thermal annealing improving crystalline quality; for higher Cd content, the quaternary phase forms exclusively after thermal annealing.

In the ***fourth*** chapter, the analysis of the optical properties of the quaternary compounds Cu_2ZnSnS_4 (CZTS) and Cu_2CdSnS_4 (CCTS) is presented, whose crystalline samples were obtained by the chemical vapor transport method, using elemental components with 99.999% purity and iodine as the transport agent. The obtained crystals had dimensions of approximately 1–2 mm × 3–5 mm and displayed a smooth optical surface, as can be seen in Fig. 14.

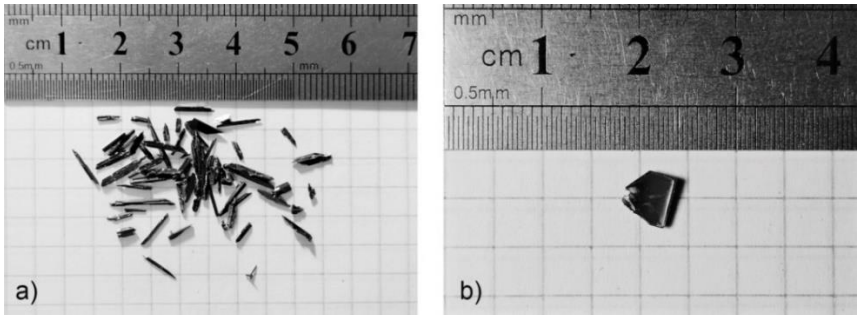

Fig. 14. Image of the single crystals obtained by the chemical vapor transport method: a) - CCTS and b) - CZTS.

The chemical composition of the samples, determined by X-ray fluorescence (XRF), indicated a deficit of Cu and Sn, as well as a high S content in both samples (Table 8). For the CZTS sample, the determined cationic ratios are Cu/(Zn+Sn) = 1.04 and Zn/Sn = 0.95, while for CCTS – Cu/(Cd+Sn) = 1.04 and Cd/Sn = 0.95. These deviations from stoichiometry can significantly influence the optical properties and the concentration of structural defects in the investigated samples.

Table 8. Chemical composition of the samples measured by the XRF method.
Note: II=Zn or Cd, M= Cu+II+Sn.

Sample	Cu (at.%)	Zn (at.%)	Cd (at.%)	Sn (at.%)	S (at.%)	Cu/ (II+Sn)	II/ Sn	M/ S
CZTS	18.4±0.07	8.6±0.05	–	9.1±0.1	63.9±0.1	1.04	0.95	0.57
CCTS	17.2±0.07	–	9.1±0.08	9.6±0.1	64.0±0.8	0.92	0.96	0.56

The reflectance and transmittance spectra of the CZTS sample, measured at 300 K, are shown in Fig. 15. Two intense maxima are observed in the reflectance spectrum, labeled A_1 and B_1, located at 1.38 and 1.70 eV respectively, assigned to direct transitions between the valence bands and the conduction band at the center of the Brillouin zone. In addition, the transmittance spectrum shows that the sample becomes opaque for energies greater than approximately 1.47 eV, indicating the proximity of the fundamental absorption edge.

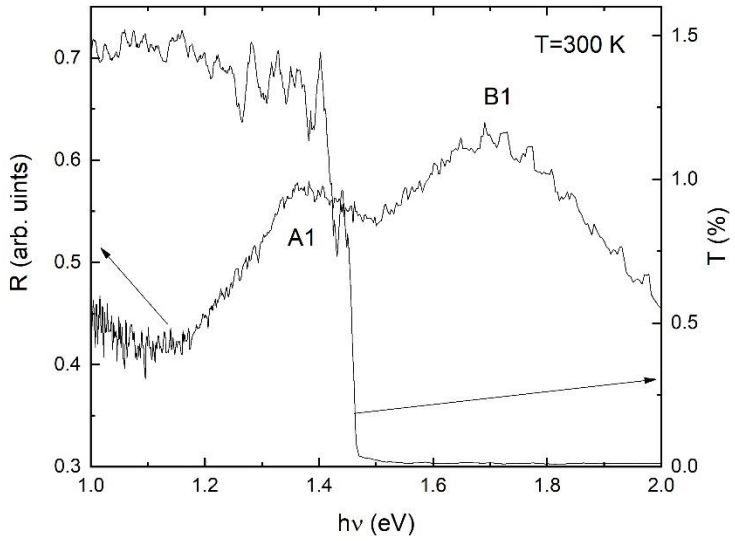

Fig. 15. Reflectance and transmittance spectra of the CZTS sample, measured at 300 K temperature.

The absorption coefficient was calculated using the expression:

$$\alpha = \frac{1}{d} ln\left(\frac{(1-R)^2}{T}\right) \quad (10)$$

where *R*, *T* and *d* represent the reflectance, transmittance and thickness of the sample. Thus, absorption begins around 1.4 eV, while the band-gap width determined by the Tauc method is ~1.46 eV at 300 K, in agreement with the results from the specialized literature [11, 12].

The reflectance spectra of the CZTS sample (Fig. 16), measured in the range 10–300 K, revealed an unusual behavior of the A_1 and B_1 maxima: their positions shift toward higher energies with decreasing temperature down to ~150 K, after which the trend reverses. This behavior suggests

that the transitions originate from the same conduction-band minimum, but from different valence-band maxima.

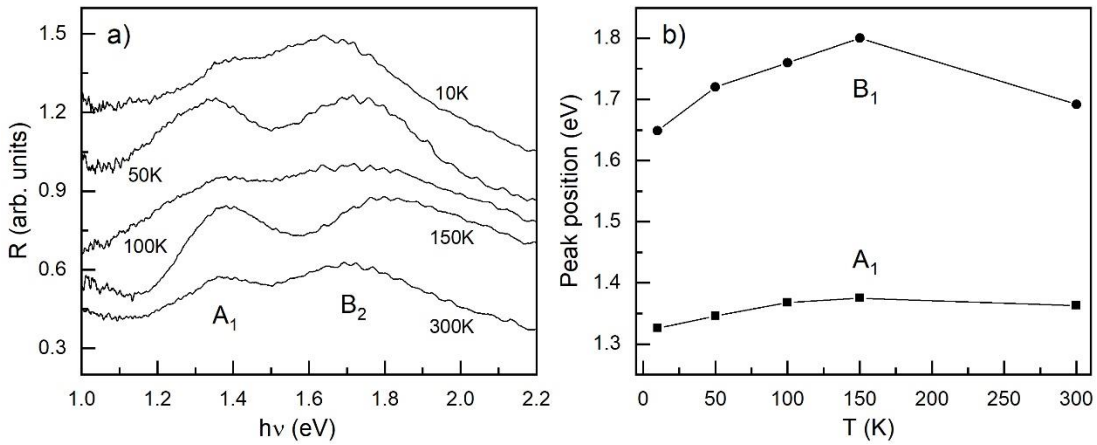

Fig. 16. a) - Reflectance spectra of the CZTS single-crystal sample, measured at different temperatures, and b) – temperature dependence of the position of the A1 and B1 maxima.

For the CCTS compound, the reflectance and photoluminescence spectra in the fundamental band-edge region were also investigated. The reflectance spectra were measured in the range 50–300 K and are shown in Fig. 17.

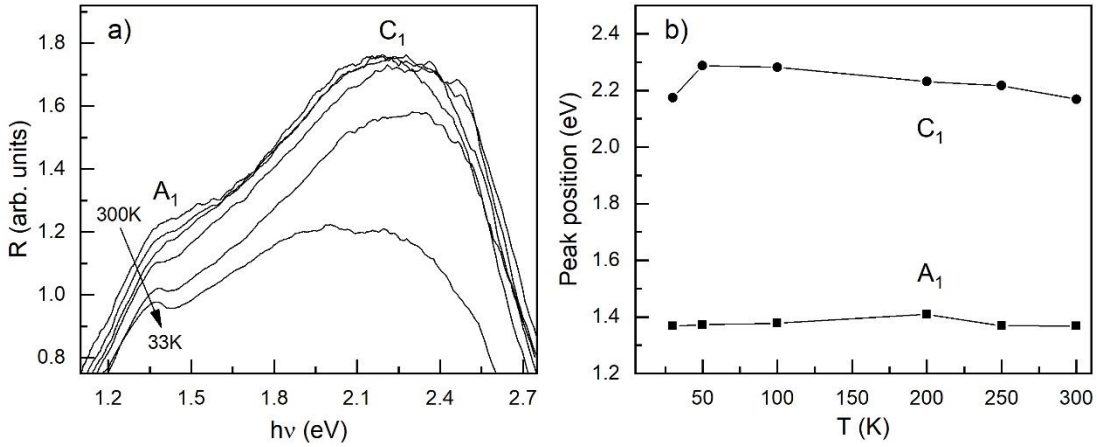

Fig. 17. a) - Reflectance spectra of the CCTS single-crystal sample, measured at different temperatures, and b) – temperature dependence of the position of the A1 and C1 maxima.

In these spectra, the A_1 maximum, located at approximately 1.37 eV, is present at all temperatures. In addition, an extra, broad and asymmetric maximum, labeled C_1, was detected around the value 2.27 eV. Unlike the CZTS sample, the B_1 maximum is not present in the CCTS sample spectra. As temperature decreases, the C_1 maximum shifts toward higher energies, a behavior

characteristic of direct transitions between the conduction and valence bands, but occurring at different points of the Brillouin zone.

The reflectance and photoluminescence spectra of the CCTS sample, measured at a temperature of 15 K (Fig. 18), allowed the identification of excitons A and B in the states $n = 1$ and $n = 2$. The first state of exciton A ($n^A = 1$) is located at 1.33 eV, while the second ($n^A = 2$) is at 1.37 eV. In addition, a narrow peak was detected around the value of 1.37 eV, associated with the longitudinal exciton ω_L, while the first state observed in the luminescence spectrum corresponds to the transverse exciton ω_T. For exciton B, the states $n^B = 1$ and $n^B = 2$ were identified at approximately 1.43 and 1.49 eV respectively.

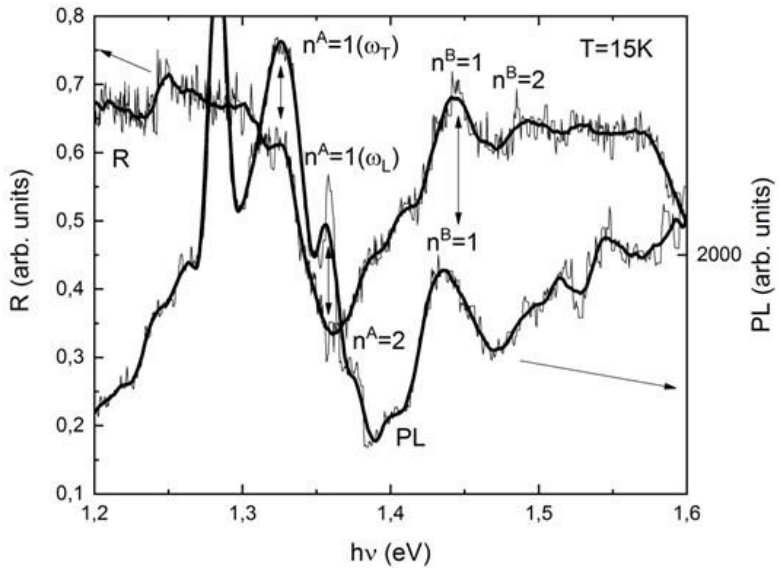

Fig. 18. Reflectance (R) and photoluminescence (PL) spectra measured at a temperature of 15 K, in the fundamental absorption-edge region of the CCTS sample.

The energy corresponding to the band gap (E_∞) and the Rydberg constant (Ry) were estimated using the expressions:

$$E_n = E_g - \frac{Ry}{n^x} \tag{11}$$

$$\mathrm{Ry} = \frac{n_2^x (E_2 - E_1)}{\left(\frac{n_2}{n_1}\right)^x - 1} \tag{12}$$

$$E_g = \frac{E_2 \left(\frac{n_2}{n_1}\right)^x - E_1}{\left(\frac{n_2}{n_1}\right)^x - 1} \tag{13}$$

where $n_1 = 1$ and $n_2 = 2$ represent the excitonic states with energies E_1 and E_2, and $x = 2$. For exciton A, $Ry \approx 64$ meV and $E_g \approx 1.39$ eV were obtained, while for exciton B, $Ry \approx 75$ meV and $E_g \approx 1.51$ eV. The difference between the energies of the two excitons confirms the existence of several valence bands near the lower edge of the band gap.

The interpretation of the experimental data was carried out based on the band diagram theoretically calculated in Ref. [13] (Fig. 19), which shows that CCTS is a direct-band-gap semiconductor, with the fundamental optical transitions occurring at the Γ point of the Brillouin zone. The diagram reveals three valence bands, V_1, V_2 and V_3, split under the action of the crystal-field and spin-orbit interaction. Exciton A was assigned to the transition between the conduction band C_1 and the valence band V_1, while exciton B was assigned to the transition between C_1 and V_2. The shape of the excitonic reflectance spectra differs considerably from the classical shape, most likely due to the screening effect induced by the high concentration of free carriers.

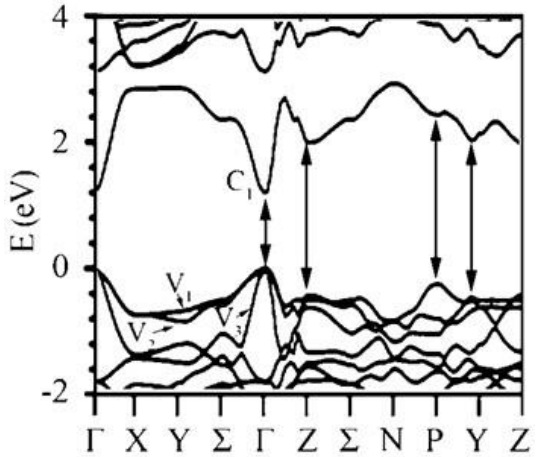

Fig. 19. Band diagram of the CCTS compound [13].

General conclusions and recommendations

General conclusions

1. Two distinct electrical conduction mechanisms were identified: nearest-neighbor hopping conduction (NNH), observed in the range ~110–190 K, and Mott-type variable-range hopping conduction (VRH), detected in the range 55–140 K.

2. The presence of the NNH mechanism is supported by the close values of the parameters E_n and W, indicating that the Fermi level is positioned near the edge of the acceptor band.

3. Analysis of the dependence of the parameters W, E_n, N/N_c and a/a_0 on composition revealed a non-monotonic behavior with a maximum for the value Cd/(Zn+Cd) ≈ 0.69, attributed to the intrinsic disorder of the investigated sample. This behavior indicates that the electrical properties depend more significantly on the presence of defects than on the chemical composition.

4. The Raman spectra obtained at 532 nm and 785 nm confirmed the presence of the quaternary phase in the samples of the end-member compounds CZTS and CCTS, in good agreement with the specialized literature. In the CCTS sample at 785 nm, an additional peak was identified at 313 cm^{-1}, assigned to the secondary SnS_2 phase.

5. The kesterite-stannite structural transition was identified in the Raman spectra of the CZCTS solid solutions: the frequency of the main peak decreases for cationic-ratio values Cd/(Zn+Cd) < 0.6 (kesterite-type structure) and remains nearly constant for Cd/(Zn+Cd) > 0.7 (stannite-type structure). The transition therefore occurs within the range 0.6 ≤ Cd/(Zn+Cd) ≤ 0.7, where the two structures coexist.

6. The Raman spectra of the non-annealed samples show three predominant bands: the main band located at 351–359 cm^{-1} (quaternary phase) and two bands at ~258 and 493 cm^{-1}, assigned to residual salts (thiourea, CuCl) or intermediate synthesis compounds.

7. The thermally treated CZCGS thin films showed the formation of a wurtzstannite-type structure for both end-member compounds (CZGS and CCGS). Additionally, the band located in the range 280–300 cm^{-1} proved to be much more sensitive to compositional changes, shifting toward lower wavenumbers as Zn is substituted with Cd.

8. In the reflectance and photoluminescence spectra of the CCTS compound, type-A excitons (n^A=1 at 1.33 eV, n^A=2 at 1.37 eV) and type-B excitons (n^B=1 at 1.43 eV, n^B=2 at 1.49 eV) were identified, with Rydberg constants of approximately 64 meV and 75 meV, respectively.

9. For CZTS, the band-gap width determined by the Tauc method at 300 K is ~1.46 eV. The unusual behavior of the maxima in the reflectance spectra suggests that the electronic transitions originate from the same conduction-band minimum, but from different valence-band maxima.

Recommendations

10. The study of the transport properties of the quaternary compounds can be used to assess the concentration of CuZn and ZnCu antisite defects, while Raman spectroscopy allows the identification of secondary phases and the assessment of sample crystallinity.

11. The synthesis conditions of the thin films should be optimized to minimize CuZn and ZnCu antisite defects, by analyzing the dependence of the concentration of these defects on the Cd content in the $Cu_2(Zn,Cd)(Sn,Ge)S_4$ compounds, with a view to identifying the optimal composition.

12. The data on optical properties can be used to assess the reflection, absorption and transmittance qualities of thin films, contributing to the determination of the optimal band-gap width for maximum photovoltaic device efficiency.

13. The quality of the Raman spectra of polycrystalline thin films can be improved by carrying out measurements on crystalline samples with a high degree of homogeneity, which would minimize the overlap between the secondary-phase peaks and those of the quaternary phase.

14. The use of additional excitation wavelengths for the Raman spectra would allow more precise identification of secondary phases and more complete conclusions regarding the dependence of the vibrational properties on chemical composition. Thus, Raman spectroscopy remains an essential technique for differentiating crystal structures and identifying the predominant phases in quaternary compounds, including in cases where this becomes difficult to achieve using X-ray diffraction.

Bibliography

1. WANG, J., MENG, F., LOU, L., YIN, K., XU, X., JIAO, M. et al. Vacancy-enhanced cation ordering via magnesium doping to enable kesterite solar cells with 14.9% certified efficiency. In: Nature Energy, 2025, vol. 11, pp. 66–75, ISSN 2058-7546.

2. LISUNOV, KG., GUK, M., NATEPROV, A., LEVCENKO, S., TEZLEVAN, V., ARUSHANOV, E. Features of the acceptor band and properties of localized carriers from studies of the variable-range hopping conduction in single crystals of p-Cu2ZnSnS4. In: Solar Energy Materials and Solar Cells, 2013, vol. 112, pp. 127–133, ISSN 09270248.

3. LÄHDERANTA, E., HAJDEU-CHICAROSH, E., SHAKHOV, MA., GUC, M., BODNAR, IV., ARUSHANOV, E. et al. Hopping magnetotransport of the band-gap tuning Cu2 Zn(Sn x Ge 1− x)Se4 crystals. In: Journal of Physics: Condensed Matter, 2016, vol. 28, p. 455801, ISSN 0953-8984, 1361-648X.

4. GUC, M., CABALLERO, R., LISUNOV, KG., LÓPEZ, N., ARUSHANOV, E., MERINO, JM. et al. Disorder and variable-range hopping conductivity in Cu2ZnSnS4 thin films prepared by flash evaporation and post-thermal treatment. In: Journal of Alloys and Compounds, 2014, vol. 596, pp. 140–144, ISSN 09258388.
5. SHKLOVSKII, BI., EFROS, AL. Electronic Properties of Doped Semiconductors. Berlin Heidelberg: Springer-Verlag, 1984. 388 p. ISBN 3-540-12995-2.
6. LÄHDERANTA, E., HAJDEU-CHICAROSH, E., KRAVTSOV, V., SHAKHOV, MA., STAMOV, VN., BODNAR, IV. et al. Electronic properties of Cu2 (Zn, Cd)SnS4 determined by the high-field magnetotransport. In: New Journal of Physics, 2022, vol. 24, p. 093008, ISSN 1367-2630.
7. GUC, M., LISUNOV, KG., HAJDEU, E., LEVCENKO, S., URSAKI, V., ARUSHANOV, E. Variable-range hopping conductivity in Cu2ZnGeSe4 single crystals. In: Solar Energy Materials and Solar Cells, 2014, vol. 127, pp. 87–91, ISSN 09270248.
8. LISUNOV, KG., GUC, M., LEVCENKO, S., DUMCENCO, D., HUANG, YS., GURIEVA, G. et al. Energy spectrum of near-edge holes and conduction mechanisms in Cu2ZnSiSe4 single crystals. In: Journal of Alloys and Compounds, 2013, vol. 580, pp. 481–486, ISSN 09258388.
9. GUC, M., LITVINCHUK, AP., LEVCENKO, S., IZQUIERDO-ROCA, V., FONTANÉ, X., VALAKH, MYa. et al. Optical phonons in the wurtzstannite Cu 2 ZnGeS 4 semiconductor: Polarized Raman spectroscopy and first-principle calculations. In: Physical Review B, 2014, vol. 89, p. 205205, ISSN 1098-0121, 1550-235X.
10. LITVINCHUK, AP., DZHAGAN, VM., YUKHYMCHUK, VO., VALAKH, MYa., BABICHUK, IS., PARASYUK, OV. et al. Electronic structure, optical properties, and lattice dynamics of orthorhombic Cu 2 CdGeS 4 and Cu 2 CdSiS 4 semiconductors. In: Physical Review B, 2014, vol. 90, p. 165201, ISSN 1098-0121, 1550-235X.
11. LEVCENKO, S., HAJDEU-CHICAROSH, E., GARCIA-LLAMAS, E., CABALLERO, R., SERNA, R., BODNAR, IV. et al. Spectroscopic ellipsometry study of Cu2ZnSnS4 bulk poly-crystals. In: Applied Physics Letters, 2018, vol. 112, p. 161901, ISSN 0003-6951, 1077-3118.
12. LI, S-Y., HÄGGLUND, C., REN, Y., SCRAGG, JJS., LARSEN, JK., FRISK, C. et al. Optical properties of reactively sputtered Cu2ZnSnS4 solar absorbers determined by spectroscopic ellipsometry and spectrophotometry. In: Solar Energy Materials and Solar Cells, 2016, vol. 149, pp. 170–178, ISSN 09270248.
13. SARMADIAN, N., SANIZ, R., PARTOENS, B., LAMOEN, D. First-principles study of the optoelectronic properties and photovoltaic absorber layer efficiency of Cu-based chalcogenides. In: Journal of Applied Physics, 2016, vol. 120, p. 085707, ISSN 0021-8979, 1089-7550.

List of the author's publications on the thesis topic

Articles in journals indexed in Web of Science and SCOPUS:

1. NWAMBAEKWE, Kelechi Chiemezie, **BATIR, Valentin,** DERMENJI, Lazari, CURMEI, Nicolai, ARUSHANOV, Ernest, EMMANUEL, Iwuoha. Spray-pyrolyzed Cd-substituted kesterite thin-films for photovoltaic applications: Post annealing conditions and property studies. In: Materials Chemistry and Physics, 2023, vol. 301, pp. 1-15. ISSN 0254-0584. DOI: https://doi.org/10.1016/j.matchemphys.2023.127594

2. **BATIR, Valentin,** ZALAMAI, Victor. Optical properties of Cu_2ZnSnS_4 and Cu_2CdSnS_4 quaternary compounds. In: Romanian Reports in Physics, 2024, vol. 76, pp. 1-13. ISSN 1221-1451. DOI: https://doi.org/10.59277/RomRepPhys.2024.76.506
3. **BATIR, Valentin,** LISUNOV, Konstantin, ARUSHANOV, Ernest. Variable-range hopping conduction in the $Cu_2Zn_{1-x}Cd_xSnS_4$ single crystals. In: Romanian Reports in Physics, 2026, vol. 78, pp. 1-12. DOI: https://doi.org/10.59277/RomRepPhys.2026.78.502
4. **BATIR, Valentin,** AAZOU, Safae, DERMENJI, Lazari, CURMEI, Nicolai, SEKKAT, Zouheir, ARUSHANOV, Ernest, GUC, Maxim. Vibrational properties of $Cu_2Zn_{1-x}Cd_xGeS_4$ solid solutions: Raman analysis and effect of thermal annealing. In: Applied Physics Letters, 2026, vol. 128, pp. 1-15. DOI: https://doi.org/10.1063/5.0325060
5. **BATIR, Valentin,** ARUSHANOV, Ernest. Effect of cadmium substitution on the structural phase transition and Raman vibrational modes of $Cu_2Zn_{1-x}Cd_xSnS_4$ solid solutions. In: Surface Engineering and Applied Electrochemistry, 2026. ISSN 1068-3755. (in press).

Participation in international scientific events:

1. **BATIR, Valentin,** HAJDEU-CHICAROSH, Elena, VIKTOROV, I. , LÄHDERANTA, Erkki, LISUNOV, Konstantin, ARUSHANOV, Ernest. Hopping conductivity in $Cu_2Zn_{1-x}Cd_xSnS_4$. In: Materials Science and Condensed Matter Physics: , dedicated to the 60th anniversary from the foundation of the Institute of Applied Physics, Ed. 10, 1-4 October 2024, Chișinău. Chișinău, Republic of Moldova: Editorial-Polygraphic Center of Moldova State University, 2024, Edition 10, p. 75. ISBN 978-9975-62-763-4. Poster.
2. **BATIR, Valentin,** AAZOU, Safae , DERMENJI, Lazari, CURMEI, Nicolai, SEKKAT, Zouheir, ARUSHANOV, Ernest, GUK, Maxim. Raman analysis of $Cu_2Zn_{1-x}Cd_xGeS_4$ and $Cu_2CdSn_{1-x}Ge_xS_4$ solid solutions. In: Materials Science and Condensed Matter Physics: , dedicated to the 60th anniversary from the foundation of the Institute of Applied Physics, Ed. 10, 1-4 October 2024, Chișinău. Chișinău, Republic of Moldova: Editorial-Polygraphic Center of Moldova State University, 2024, Edition 10, p. 84. ISBN 978-9975-62-763-4. Poster.

Participation in national scientific events with international participation:

1. **BATIR, Valentin,** ZALAMAI, Victor, ARUSHANOV, Ernest. Optical properties of Cu_2ZnSnS_4 and Cu_2CdSnS_4 quaternary compounds. In: Natural sciences in the dialogue of generations, Ed. 7, 12-13 September 2024, Chişinău. Chişinău: Editorial-Polygraphic Center of Moldova State University, 2024, Edition 7, p. 240. ISBN 978-9975-62-756-6. Communication.

Participation in national scientific events:

1. **BATIR, Valentin.** Optical properties of the quaternary compounds Cu_2ZnSnS_4 și Cu_2CdSnS_4. In: National Scientific Conference of Doctoral Students “Contemporary Research and Evaluation Methodologies” 22-23 April 2021, Chişinău. Communication.

Adnotare

Batîr Valentin

„Proprietăți de transport, vibraționale și optice ale soluțiilor solide $Cu_2(Zn,Cd)(Sn,Ge)S_4$”

Teză de doctor în științe fizice, Chișinău, anul 2026

Teza este scrisă în limba română şi constă din introducere, patru capitole, concluzii generale și recomandări, bibliografie din 185 de lucrări citate. Lucrarea conține 126 pagini de text, 50 figuri, 18 tabele şi 44 formule.

Cuvinte-cheie: proprietăți electrice, kesterit, stanit, wurtzstanit, CZTS, CCTS, CZCTS, soluții solide, densitate de stări, conductibilitate prin salturi, fantă Coulomb, bandă acceptoare, proprietățile vibraționale, spectroscopia Raman, reprezentare ireductibilă, tranziție structurală kesterit-stanit, dezordine structurală, interacțiune interatomică, lățimea benzii interzise, coeficient de absorbție, stoichiometrie, cationi, faze secundare, rețea cristalină, compus calcogenid, tratare termică.

Scopul principal al tezei reprezintă stabilirea corelației dintre parametrii fizico-chimici principali și compoziția soluțiilor solide $Cu_2(Zn,Cd)(Sn,Ge)S_4$ prin studiul fundamental al proprietăților de transport, vibraționale și optice ale acestor compuși.

Obiectivele cercetării: Determinarea mecanismelor de transport electric predominante în compușii CZCTS la diferite temperaturi. Înregistrarea spectrelor Raman caracteristice compușilor CZCTS și $Cu_2(Zn,Cd)GeS_4$, în scopul investigării proprietăților vibraționale și îmbunătățirii calității probelor. Stabilirea parametrilor și tranzițiilor optice în compușii Cu_2ZnSnS_4 și Cu_2CdSnS_4 pe baza spectrelor de reflectanță, transmitanță și fotoluminescență.

Noutatea și originalitatea științifică a tezei constă în investigarea în premieră a proprietăților de transport ale soluțiilor solide $Cu_2Zn_{1-x}Cd_xSnS_4$ în intervalul de valori $0 \leq x \leq 1$. De asemenea a fost propus în premieră un model liniar pentru evaluarea rapidă a compoziției soluțiilor solide CZCTS și $Cu_2(Zn,Cd)GeS_4$, bazat pe spectrele Raman caracteristice ale acestor compuși semiconductori. Totodată, în spectrele de fotoluminescență și reflectanță ale compusului Cu_2CdSnS_4, măsurate la temperatura de 15 K, au fost identificați și analizați pentru prima dată excitonii de tip A și B.

Rezultatele obținute care contribuie la soluționarea unei probleme științifice importante sunt reprezentate de determinarea diferitor parametri caracteristici proprietăților de transport, vibraționale, optice și construirea dependențelor acestor parametri de compoziția probelor. Acest lucru poate fi important pentru determinarea unei compoziții optime a stratului absorbant, care va permite fabricarea dispozitivelor fotovoltaice cu eficiență sporită.

Semnificația teoretică și valoarea aplicativă a rezultatelor obținute rezidă în extinderea fondului de cunoștințe referitoare la proprietățile fundamentale ale compușilor $Cu_2(Zn,Cd)(Sn,Ge)S_4$ și aplicarea acestor cunoștințe pentru fabricarea dispozitivelor fotovoltaice economic accesibile, pe baza straturilor subțiri ale compușilor investigați.

Implementarea rezultatelor științifice: Rezultatele obținute în cadrul tezei de doctor au fost utilizate la realizarea mai multor proiecte de cercetare și vor putea fi de asemenea valorificate în practică la proiectarea diferitor dispozitive fotovoltaice și optoelectronice pe baza materialelor $Cu_2(Zn,Cd)(Sn,Ge)S_4$.

Summary

Batîr Valentin

„Transport, vibrational and optical properties of solid solutions $Cu_2(Zn,Cd)(Sn,Ge)S_4$"

Thesis for degree of Doctor of Philosophy in Physical Sciences, Chişinău, 2026

The thesis is written in Romanian and consists of an introduction, four chapters, general conclusions and recommendations, bibliography of 185 cited works. The work contains 126 pages of text, 50 figures, 18 tables and 44 formulas.

Keywords: electrical properties, kesterite, stannite, wurtzstannite, CZTS, CCTS, CZCTS, solid solutions, density of states, hopping conductivity, Coulomb gap, acceptor band, vibrational properties, Raman spectroscopy, irreducible representation, kesterite–stannite structural transition, structural disorder, atomic interaction, absorption coefficient, stoichiometry, cations, secondary phases, crystal lattice, chalcogenide compound, annealing.

The main goal of the thesis is to establish the correlation of the main physicochemical properties of $Cu_2(Zn,Cd)(Sn,Ge)S_4$ solid solutions with their chemical composition by analysis of the fundamental transport, vibrational and optical properties of these compounds $Cu_2(Zn,Cd)(Sn,Ge)S_4$.

Research objectives: To define the main electrical charge transfer mechanisms in CZCTS solid solution at different temperatures. To establish characteristic Raman spectra of CZCTS and $Cu_2(Zn,Cd)GeS_4$ solid solutions, to analyze vibrational properties and assess phase quality and homogeneity. To define main optical parameters and optical transitions in Cu_2ZnSnS_4 and Cu_2CdSnS_4 quaternary compounds at different temperatures by means of reflectance, transmittance and photoluminescence spectroscopies.

The scientific novelty and originality of the thesis consist in the first detailed analysis of the electrical charge transfer in $Cu_2Zn_{1-x}Cd_xSnS_4$ solid solutions in the range of values $0 \leq x \leq 1$ by applying different theoretical models. Also, a characteristic spectrum of CZCTS and $Cu_2(Zn,Cd)GeS_4$ solid solutions was established allowing to propose a novel method for the fast evaluation of the composition with the change of Cd/(Zn+Cd) ratio in these solid solutions. At the same time, excitons of type A and B were observed and analyzed for the first time in Cu_2CdSnS_4 compound by means of photoluminescence and reflectance spectroscopy.

Obtained results that contribute to solving of an important scientific problem consist in the determination of characteristic parameters of the transport, vibrational and optical properties, and defining the dependences of these properties on the chemical composition of the samples. This provides a basis for identifying optimal composition of absorber layer with the desired physicochemical properties for applications in thin film solar cells.

The theoretical significance and applicative value of the obtained results reside in the expansion of the knowledge data base regarding the fundamental properties of the $Cu_2(Zn,Cd)(Sn,Ge)S_4$ compounds and the application of this knowledge for the manufacture of low-cost and environmentally friendly photovoltaic devices.

Implementation of scientific results: The results obtained within the doctoral thesis were used in performing of several research projects and can be used in the design of various photovoltaic and optoelectronic devices based on $Cu_2(Zn,Cd)(Sn,Ge)S_4$ compounds.

Аннотация
Батыр Валентин
„Транспортные, колебательные и оптические свойства твердых растворов $Cu_2(Zn,Cd)(Sn,Ge)S_4$”
Кандидатская диссертация по физическим наукам, Кишинев, 2026 год

Диссертация написана на румынском языке и состоит из введения, четырех глав, общих выводов и рекомендаций, библиографии из 185 цитируемых работы. Диссертация содержит 126 страниц текста, 50 рисунка, 18 таблицы и 44 формулы.

Ключевые слова: электрические свойства, кестерит, станнит, вюрцстаннит, CZTS, CCTS, CZCTS, твердые растворы, плотность состояний, прыжковая проводимость, кулоновская щель, акцепторная полоса, спектры Рамана, неприводимое представление, структурный переход кестерит-станнит, структурный беспорядок, межатомное взаимодействие, коэффициент поглощения, стехиометрия, катионы, вторичные фазы, кристаллическая решетка, халькогенидное соединение, отжиг.

Основная цель диссертации – фундаментальное исследование транспортных, колебательных и оптических свойств соединений $Cu_2(Zn,Cd)(Sn,Ge)S_4$ с целью установления корреляции между основными параметрами, характеризующими эти свойства, и химическим составом образцов.

Задачи исследования: выявление механизмов переноса заряда в твёрдых растворах CZCTS в широком температурном диапазоне; получение характерных Рамановских спектров соединений $Cu_2(Zn,Cd)SnS_4$ и $Cu_2(Zn,Cd)GeS_4$ для изучения колебательных свойств и повышения фазовой однородности образцов; определение основных оптических параметров и переходов в соединениях Cu_2ZnSnS_4 и Cu_2CdSnS_4 по спектрам отражения, пропускания и фотолюминесценции при различных температурах.

Научная новизна и оригинальность диссертации: впервые измерены транспортные свойства твёрдых растворов $Cu_2(Zn,Cd)SnS_4$ во всём интервале $0 \leq x \leq 1$; предложена линейная модель быстрой оценки состава $Cu_2(Zn,Cd)GeS_4$ на основе Рамановских спектров; впервые проанализированы экситоны типов A и B в спектрах фотолюминесценции и отражения четверного соединения Cu_2CdSnS_4.

Полученные результаты, которые способствуют решению важной научной проблемы заключаются в определении ключевых транспортных, колебательных и оптических параметров в зависимости от состава образцов, что позволяет выбрать оптимальный состав поглощающего слоя для фотоэлектрических устройств.

Теоретическая и прикладная ценность работы заключается в расширении базы знаний о фундаментальных свойствах соединений $Cu_2(Zn,Cd)(Sn,Ge)S_4$ и применении этих знаний для создания доступных фотоэлектрических устройств на основе тонких плёнок. Результаты использованы в нескольких исследовательских проектах и применимы при проектировании фотоэлектрических и оптоэлектронных устройств.

BATÎR Valentin

TRANSPORT, VIBRATIONAL AND OPTICAL PROPERTIES OF $Cu_2(Zn,Cd)(Sn,Ge)S_4$ SOLID SOLUTIONS

134.01 – Physics and technology of materials

Summary of the doctoral thesis in physical sciences

Approved for printing: 04.08.2026
Offset paper:
Print sheets: 2.0

Paper size: 60×84 1/16
Type offset: 35 copies
Order nr. 65/26

Editorial – Polygraphic Center of Moldova State University
Str. A. Mateevici 60, MD - 2009, Chisinău